https://doi.org/10.32604/zkg.2024.05.01

Effect of Al_2O_3 on NO_x and SO_2 of RDF combustion

Zhengming Yi[1,2], Zihang Zhou[1,2], Juan Zhou[1,2], Lichen Shi[1,2] and Xiaolin Chen[1,2]
[1]State Key Laboratory of Refractories and Metallurgy, Wuhan University of Science and Technology, Wuhan / China;
[2]Key Laboratory for Ferrous Metallurgy and Resources Utilization of Ministry of Education, Wuhan University of Science and Technology, Wuhan / China
*Corresponding author: chenxiaolin@wust.edu.cn

ABSTRACT: The formation of gas products (NO_x and SO_2) in the combustion of RDF and 0.00 g, 0.02 g, 0.04 g, and 0.08 g Al_2O_3 at 900 °C was studied by using the experimental platform of a double-tube furnace set up in the laboratory. The results show that mixing Al_2O_3 can inhibit the formation of volatile NO_x, but promote the formation of fixed carbon NO_x. Al_2O_3 can inhibit the increase of total NO_x formation during RDF combustion. Al_2O_3 has a good effect on removing SO_2 in the RDF combustion process. When the mixing amount of Al_2O_3 is 0.00 g, the total amount of SO_2 generated is 0.39 mg, and when the mixing amount of Al_2O_3 is 0.08 g, the total amount of SO_2 generated is 0.29 mg, that is, Al_2O_3 is a good desulfurizing agent.

1 Introduction

The total annual production of municipal solid waste in China increased from 31.3 million tons (1980) to 343 million t (2019) and could reach 480 million t by 2030 [1]. RDF (Refuse-derived fuel) is a fuel derived from the sorting, crushing, drying, and processing of refuse, which has high calorific value, stable combustion, and low dioxin emission [2–4]. Therefore, RDF can be used as a good alternative fuel for fi ring cement [5–7]. The utilization of MSW into RDF is not only conducive to the reuse of resources, but also reduces environmental pollution. Nowadays, the national and local governments actively encourage the use of cement kilns for collaborative disposal of RDF, which provides a new idea for the efficient disposal of municipal solid waste [8]. When RDF is used as an alternative fuel in cement kilns, it will inevitably be affected by complex raw material components. Studying the effects of raw material components on the RDF combustion process is of great significance for exploring the emission mechanism of NO_x, SO_2, and other pollutants when RDF is used as an alternative fuel.

Metal oxides have great influence on the formation of NO_x and SO_2 during RDF combustion. There have been some researches on the effect of metal oxides on the combustion process of solid fuels. Liu and Gao [9,10] analyzed the influence mechanism of metallurgical dust on NO emission in the coal combustion system, and the results showed that with the increase of the mass percentage of metallurgical dust, the peak value of NO emission decreased. Qi [11] studied the effects of mixtures ($NH_4H_2PO_4$, $CaCO_3$, and CaO) on the emission of NO and SO_2 in different coke combustion processes. The results showed that with the increase of the three mixtures, the emission of NO was enhanced to varying degrees, while the emission of SO_2 was significantly inhibited. This indicates that metal oxides have different action mechanisms on the peak value and total amount of NO produced in solid fuel. Shao and Sun [12,13] studied the catalytic pyrolysis of metal oxides on sludge and other samples, and the analysis showed that Al_2O_3 could shorten the total pyrolysis time of sludge, while CaO could extend the total pyrolysis time of sludge.

Al_2O_3 is an important raw material component in cement kilns, and it is important to study the mechanism of NO_x and SO_2 in the RDF combustion process. Fang and Liu [14–16] used thermogravimetric analysis (TGA) to study the influence of Al_2O_3 on the pyrolysis characteristics and activation energy of municipal solid waste (MSW) in N_2 atmosphere. The results showed that after adding Al_2O_3, residue quality decreased, pollutant emission decreased, aliphatic hydrocarbon ratio increased, oxygen-containing compound ratio decreased, and activation energy decreased.

However, studies on the mechanism of metal oxides in coal combustion are common at present, while studies on the co-combustion of metal oxides and RDF are rarely reported. Meanwhile, the interaction between gas components such as CO, NO_x, SO_2 in RDF combustion remains unclear. In this paper, the environment of the precalciner is simulated by the double-tube furnace reactor platform built in the laboratory. High-temperature combustion experiments were carried out on the mixed samples of RDF and Al_2O_3 of 0.00 g, 0.02 g, 0.04 g, and 0.08 g, and the influence of Al_2O_3 on the generation and transformation of CO, NO_x, SO_2 and other gases in the combustion process of RDF was quantitatively and qualitatively studied.

MATERIALS

2 Materials and Methods

2.1 Raw materials

The experimental raw materials used in this study were RDF and Al_2O_3. The alternative fuel chosen for the RDF is the actual alternative fuel used by a cement company in Hubei, which comes from municipal household waste in Wuhan. The industrial analysis of RDF is carried out concerning the national standard (GB/T 212-2008). Elemental analysis by determination of the elemental content of C, H, O, N, and S in the fuel using a Vatio EL cube elemental analyzer from Elemental Analysis Systems, Germany. The calorific value was determined three times using an oxygen bomb calorimeter and the average value was taken. Table 1 shows the industrial analysis, elemental analysis and calorific values of the RDF used in the experiments. Al_2O_3 is produced by Tianjin Zhiyuan Chemical Reagent Co., Ltd. and the content of Al_2O_3 is ≥ 98.0%.

2.2 Experimental apparatus and methods

2.2.1 Tube furnace combustion experiments

The simulated combustion experimental system is shown in Figure 1, with a tube furnace model OTF-1200X and an adjustable temperature range: room temperature to 1200 ˚C. The combustion atmosphere is prepared by N_2/O_2 and the flue gas components of the specimen after combustion are collected online using an MRU NOVA PLUS flue gas analyzer from Germany.

Connect the experimental device as shown in Figure 1, turn on the flue gas analyzer, and preheat it for 30~40 min. After the flue gas analyzer has started up properly and entered the monitoring interface, the entire reaction system is ventilated for a gas tightness check. Set the high-temperature tube furnace to heat up to 900 ˚C at a rate of 10 °C/min and hold. Weigh 0.5 g of RDF and different masses of Al_2O_3, mix well and lay flat in a corundum porcelain boat of size 60 mm x30 mm x15 mm. Open the gas cylinder, adjust the gas distribution cabinet to set the flow rate, set the N_2 gas flow rate to 1000 ml/min, O_2 gas flow rate to 180 ml/min, and ventilate for 10~20 min. After the gas display on the flue gas analyzer has stabilized the porcelain boat with the sample in place is quickly pushed to the middle of the high-temperature tube furnace and continuous measurement begins until the results for CO and NO_x are 0 and the data on the flue gas analyzer returns to the set gas flow density, when the recording stops. Each set of experiments was repeated three times and the mean was taken as the final result. Where CO, NO_x, and SO_2 are measured in ppm. The yields of CO, NO_x, and SO_2 can be calculated separately from equation (1) by integration of the gas curves with time as follows.

$$m_j = \sum_{i=1}^{n} c_i \times 10^{-6} \times v \div 60 \times t \times M_j \div 22.4 \quad (1)$$

where m_j is the yield of CO, NO_x, and SO_2 (mg), c_i is the concentration of CO, NO_x, and SO_2 (ppm), v is the volume flow rate 1000 (ml/min), M_j is the molar mass of CO, NO_x, and SO_2, t is the sampling interval 1 (s), n is the number of points measured, and j is CO, NO_x, and SO_2.

3 Results and Discussion

3.1 Analysis of RDF combustion at 900 ˚C

By analyzing the generation of gas products when RDF is burned in an atmosphere with O_2 concentration of 18%, it can be seen that the release curve of CO with time has two peaks, and the time of occurrence is 21 s and 262 s in turn. According to the carbon combustion mechanism, the two CO release peaks correspond to the peaks of volatile and fixed carbon precipitation in the fuel, so the two CO peaks are defined as volatile CO peak and fixed carbon CO peak. NO_x release curve over time forms two release peaks, which can be defined as volatile NO_x peak and fixed carbon NO_x peak according to the carbon combustion mechanism.

1 Proximate analysis and ultimate analysis of RDF

Sample	Proximate analysis [%]				Ultimate analysis [%]					$Q_{net} \cdot d_{af}$ /[MJ·kg^{-1}]
	Mad	FCad	Aad	Vad	Cdaf	Hdaf	Odaf	Ndaf	Sdaf	
RDF	1.13	9.11	17.93	71.83	41.94	6.45	36.30	2.26	0.39	14.54

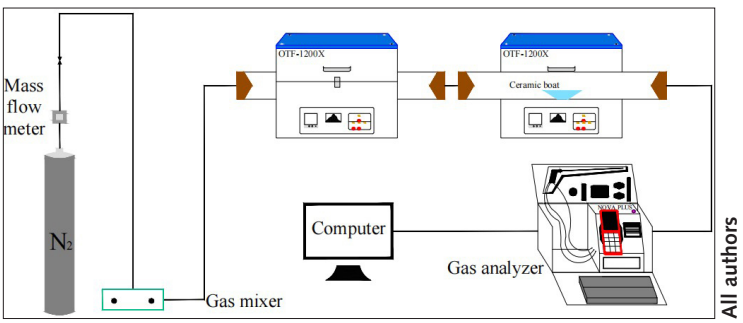

1 Diagram of the experimental system of tubular furnace reactor

The volatile NO_x peak appears earlier (t= 44 s) and has a larger peak; the fixed carbon NO_x peak appears later (t= 270 s) and has a smaller peak. Both peaks are in the form of a parabola. The release curve of SO_2 over time also takes the form of a "parabola", and its peak time is 41 s. It can be seen from the analysis of Figure 2 that during RDF combustion, the peaks of volatile CO, volatile NO_x, and SO_2 peaks appear at similar times, and all peak within 60 s after the reaction begins. The peak times of fixed carbon CO peak and fixed carbon NO_x peak are also similar, and the peak time is about 270 s. At the same time, the peaks of volatile CO and volatile NO_x are also higher than those of fixed carbon CO and fixed carbon NO_x, which is because the volatile content of RDF accounts for 71.83% (Tab. 1). Under the condition of sufficient oxygen, volatile content in RDF can be rapidly burned to produce a large amount of volatile CO and volatile NO_x.

3.2 Effect of Al_2O_3 on the formation pattern of CO, NO_x and SO_2 of RDF combustion products

Figure 3 shows the release curve of CO, NO_x, and SO_2 over time when RDF is burned at 900 °C and mixed with different Al_2O_3 masses. Table 2 shows the peak concentration and formation time of CO, NO_x and SO_2 when RDF is burned at 900 °C with different Al_2O_3 masses mixed. Figure 4 shows the total amount of CO, NO_x and SO_2 generated when RDF is burned at 900 °C and mixed with different Al_2O_3 masses.

As can be seen from Figure 3 (a), two release peaks of CO are formed when RDF is burned at 900 °C under different Al_2O_3 mixtures, namely volatile CO peak and fixed carbon CO peak. The peak value of volatile CO decreases first and then increases with the increase of Al_2O_3 mixing amount. That is, when the mixing amount of Al_2O_3 is 0.00 g, the maximum peak value of volatile CO appears at 20 ppm, and the peak time is 21 s. At the same time, the peak time of volatile CO is 21 s when mixed with different quality Al_2O_3, so it can be concluded that mixed Al_2O_3 has little influence on the formation time of volatile CO peak. The peak value of fixed carbon-type CO showed a decreasing trend with the increase of Al_2O_3 mixing amount, and the maximum peak value of fixed carbon-type CO appeared when the mixing amount of Al_2O_3 was 0.00 g. The peak formation time of fixed carbon-type CO mixed with Al_2O_3 is significantly shortened (about 10 s in advance), but the peak value of fixed carbon-type CO is little affected by the mixing amount of Al_2O_3, and the peaks are small. Combined with Figure 4(a), the total amount of CO generated shows a decreasing trend with the increase of Al_2O_3 mixing mass. When the mixing amount of Al_2O_3 is 0.04 g and 0.08 g, the minimum value of the total amount of CO generated is 0.012 mg, which is because the mixing of Al_2O_3 will increase the contact area between RDF and O_2. As a result, more CO_2 is generated, reducing the total amount of CO produced and promoting combustion.

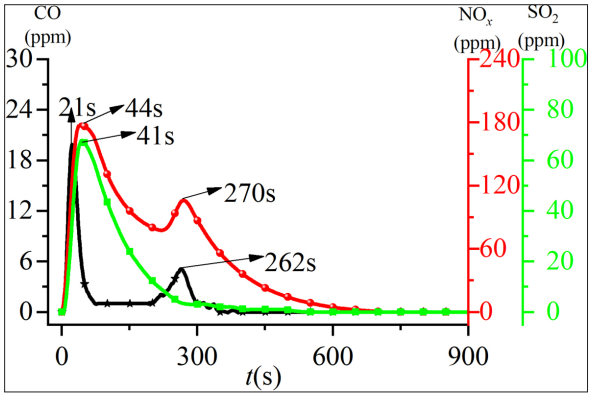

2 Variation curves of CO, NO_x, and SO_2 with time for RDF combustion at 900 °C

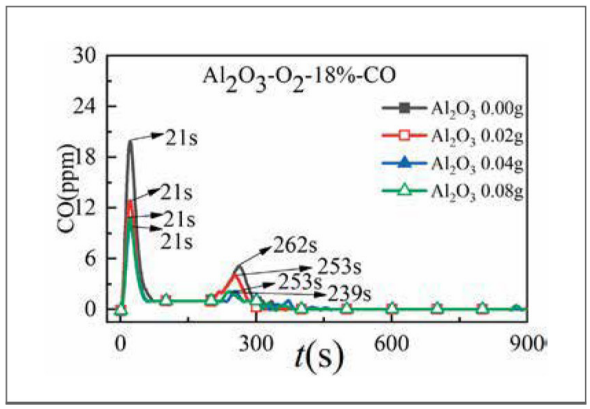

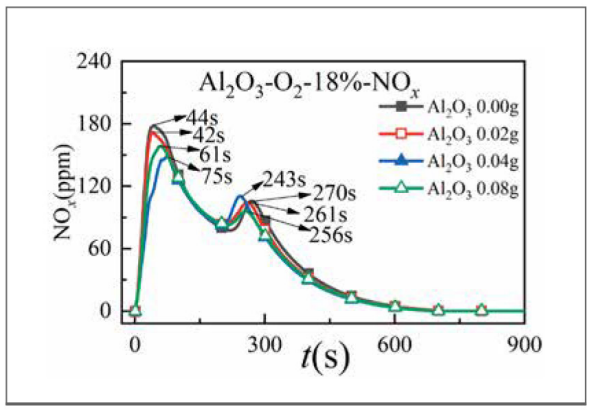

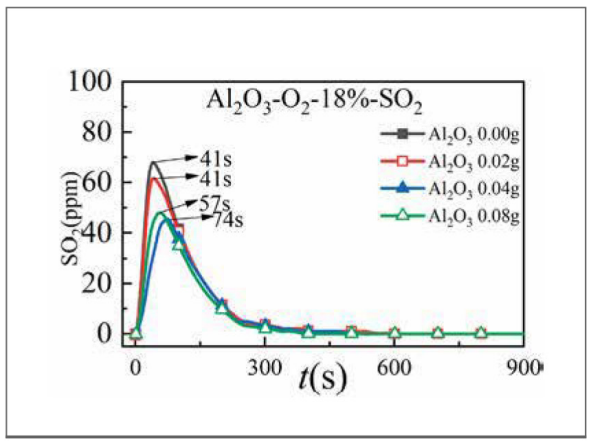

3 900 °C release curve of CO, NO_x and SO_2 over time when RDF is burned with different Al_2O_3 masses mixed

2 The peak of CO, NO_x, and SO_2 concentrations and formation times for the combustion of RDF at 900 °C

Al_2O_3		0.00 g		0.02 g		0.04 g		0.08 g	
		1st	2nd	1st	2nd	1st	2nd	1st	2nd
CO	t [s]	21	262	21	253	21	253	21	239
	Peak [ppm]	20	5	13	4	10	2	11	2
NO_x	t [s]	44	270	42	261	75	243	61	256
	Peak [ppm]	178	106	172	104	148	110	158	96
SO_2	t [s]	41	/	41	/	74	/	57	/
	Peak [ppm]	68	/	62	/	45	/	4	/

As can be seen from Figure 3(b), two release peaks are formed in the NO_x release curve over time when RDF is burned with different Al_2O_3 masses, namely volatile NO_x peak and fixed carbon NO_x peak. Both volatile NO_x peak and fixed carbon NO_x peak present a high and narrow "parabola" form. The peak of volatile NO_x is rapidly generated and released in the early stage of RDF combustion, and the peak time is 44 s, 42 s, 75 s, 61 s, and almost completely appears within 100 s after the start of combustion. The peak value of volatile NO_x decreases first and then increases with the increase of Al_2O_3 mixing amount. When the mixing amount of Al_2O_3 is 0.00 g, the maximum release peak of NO_x is 178 ppm, and when the mixing amount of Al_2O_3 is 0.04 g, the minimum release peak of NO_x is 148 ppm. The peak value of fixed carbon NO_x shows an irregular trend with the increase of Al_2O_3 mixing amount. Meanwhile, the peak formation time of fixed carbon NO_x is greatly affected by Al_2O_3, among which, the peak value is first reached when the mixing amount of Al_2O_3 is 0.04g, and the peak time is 243 s. By analysing the total amount of NO_x generated in Figure 4(b), it can be concluded that when the mixing amount of Al_2O_3 is 0.04 g, the minimum amount of NO_x generated is 0.83 mg, and when the mixing amount of Al_2O_3 is 0.00 g, the maximum amount of NO_x generated is 0.93 mg. This may be the result of the combustion of Al_2O_3 as an amphoteric oxide against RDF. However, when the mixing amount of Al_2O_3 is 0.04g, the total amount of NO_x generated is at least 0.83mg. Combined with the total amount of Figure 4(a) CO generated, it can be seen that the total amount of CO generated at this time is the least. Therefore, when the mixing amount of Al_2O_3 is 0.04 g, the reduction reaction of NO_x is the most intense, resulting in the least total amount of CO and NO_x generated. At the same time, when the mixing amount of Al_2O_3 is 0.08 g, the total amount of NO_x generation increases to 0.86 mg, which is caused by the influence of coating.

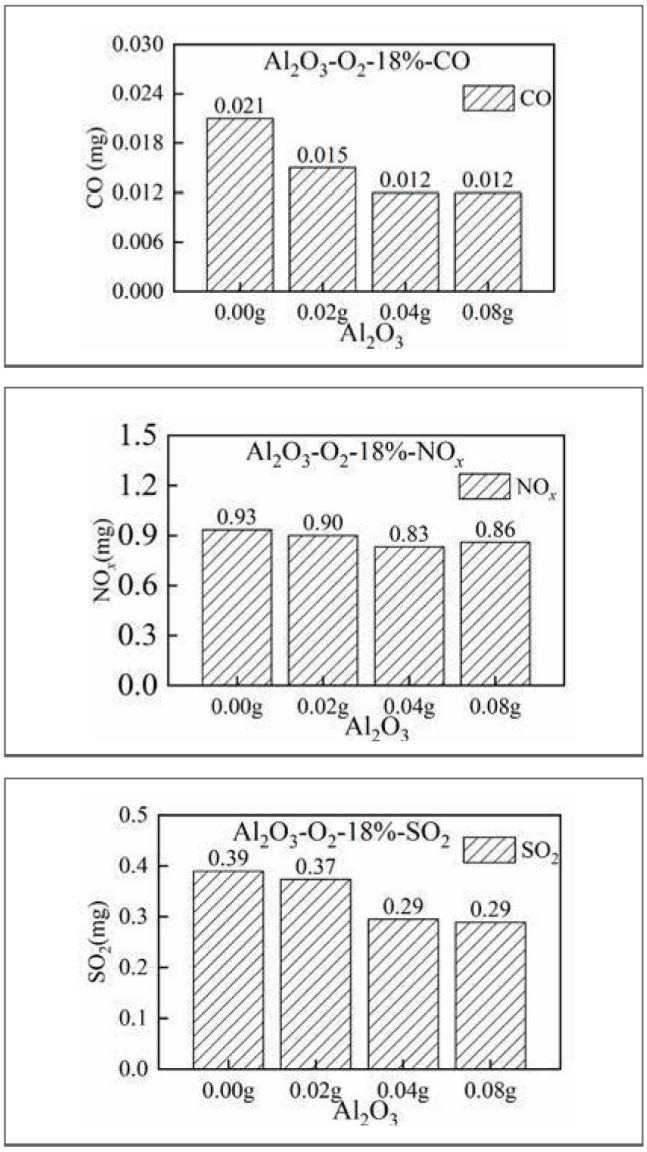

4 Total amount of CO, NO_x and SO_2 produced when RDF is burned with different Al_2O_3 masses at 900 °C

In summary, the peak value of volatile NO_x decreases first and then increases with the increase of Al_2O_3 mixing amount, while the peak value of fixed carbon NO_x shows an irregular trend with the increase of Al_2O_3 mixing amount. When the mixing amount of Al_2O_3 is 0.04g, the total amount of NO_x generated is at least 0.83 mg, so mixing the right amount of Al_2O_3 can reduce the total amount of NO_x generated.

It can be seen from Figure 3(c) that the release curve of SO_2 over time when RDF burns under different Al_2O_3 masses is in the form of a "parabola", and the release peak of SO_2 gradually decreases with the increase of the mixing amount of Al_2O_3, that is, when the mixing amount of Al_2O_3 is 0.00 g, the maximum release peak of SO_2 is 68 ppm. When the mixing amount of Al_2O_3 is 0.08 g, the

minimum release peak of SO_2 is 48 ppm, which is because Al_2O_3, as a metal oxide, acts as an absorbent and forms aluminum sulfate, thus reducing the release amount of SO_2. At the same time, the peak time of SO_2 is 41 s, 41 s, 74 s, and 57 s successively, which indicates that the SO_2 generation rate in the RDF combustion process will be inhibited with the mixing of Al_2O_3, thus reducing the combustion speed of RDF.

In summary, the release curve of SO_2 from Al_2O_3 to RDF combustion shows a regular change, that is, the peak value of SO_2 and the total amount of SO_2 are constantly decreasing with the increase of Al_2O_3 mixing amount.

4. Conclusion

(1) The mixing of Al_2O_3 will reduce the release peak value of volatile CO and fixed carbon CO, among which the release peak value of fixed carbon CO is small, and the total amount of CO generated is the least when the mixing amount of Al_2O_3 is 0.04 g and 0.08 g. Mixing Al_2O_3 will increase the contact area between RDF and O_2, thus generating more CO_2, reducing the total amount of CO generation and promoting combustion.

(2) The mixing of Al_2O_3 will reduce the peak release of volatile NO_x. The maximum peak value of fixed carbon NO_x appears when the mixing amount of Al_2O_3 is 0.00 g and the minimum peak value of fixed carbon NO_x appears when the mixing amount of Al_2O_3 is 0.04 g. In the combustion process, mixed Al_2O_3 can inhibit the increase of the total amount of NO_x generation, and 0.04 g Al_2O_3 can best inhibit the increase of the total amount of NO_x generation.

(3) The SO_2 release curve of Al_2O_3 for RDF cracking shows regular changes, that is, with the increase of Al_2O_3 mixing amount, the peak value of SO_2 and the total amount of SO_2 are constantly decreasing, which can provide certain guidance for SO_2 emission reduction of industrial cement furnace.

REFERENCES

[1] Fan, J.; Hong, H.; Zhang, L. et al.: Thermodynamic performance of SNG and power coproduction from MSW with recovery of chemical unreacted gas, Waste Management, 2017, 67: pp.163-170

[2] Yi, Z, M.; Shi, L, C.; Chen, X, L.: Effect of Cement Kiln Collaborative Disposal of Refuse Derived Fuel on the Generation and Transformation of NO_x and SO_2, Bulletin of the Chinese Ceramic Society, 2021, 40(05): pp. 1631-1637

[3] Yi, Z.; Shi, L.; Chen, X.: Effect of raw material components on RDF pyrolysis gas products, ZKG Cement Lime Gypsum, 2021(8): 74

[4] Gałko, G.; Mazur, I.; Rejdak, M. et al.: Evaluation of alternative refuse-derived fuel use as a valuable resource in various valorised applications, Energy, 2023, 263: 125920

[5] Shehata, N.; Obaideen, K.; Sayed, E, T.: Role of refuse-derived fuel in circular economy and sustainable development goals, Transactions of The Institution of Chemical Engineers. Process Safety and Environmental Protection, Part B, 2022: 163

[6] Karpan, B.; Raman, A.; Aroua, M.: Waste-to-Energy: Coal-Like Refuse Derived Fuel from Hazardous Waste and Biomass Mixture, Process Safety and Environmental Protection, 2021, 149

[7] Chen, X, L.; Xie, J, L.; Mei, S, X. et al. RDF pyrolysis by TG-FTIR and Py-GC/MS and combustion in a double furnaces reactor, Journal of Thermal Analysis and Calorimetry, 2018, 136(2): pp. 893-902

[8] Sununta, N.; Sedpho, S.; Gheewala, S, H. et al.: Life cycle greenhouse gas evaluation of organic rankine cycle using refuse-derived fuel from municipal solid waste, Journal of Renewable and Sustainable Energy, 2017, 9(5)

[9] Liu, Q.; Hu, H.; Zhou, Q. et al.: Effect of inorganic matter on reactivity and kinetics of coal pyrolysis, Elsevier Ltd, 2004: pp. 713-718

[10] Gao, Z, F.; Long, H, M.; Chun, T, J. et al.: Effect of metallurgical dust on NO emissions during coal combustion process, Journal of Iron and Steel Research International, 2018, 25(1): pp. 19-27

[11] Qi, J.; Han, K.; Wang, Q. et al.: Carbonization of biomass: Effect of additives on alkali metals residue, SO2 and NO emission of chars during combustion. Energy, 2017, 130: pp. 560-569

[12] Shao, J.; Yan, R.; Chen, H. et al.: Catalytic effect of metal oxides on pyrolysis of sewage sludge, Fuel Processing Technology, 2010, 91(9): pp. 1113-1118

[13] Sun, Y.; Chen, J.; Zhang, Z.: General roles of sludge ash, CaO and Al_2O_3 on the sludge pyrolysis toward clean utilizations, Applied Energy, 2019, pp. 233-234:412-423

[14] Fang, S.; Yu, Z.; Lin, Y. et al.: Effects of additives on the co-pyrolysis of municipal solid waste and paper sludge by using thermogravimetric analysis, Bioresource Technology, 2016, 209: pp. 265-272

[15] Fang, S.; Yu, Z.; Ma, X. et al.: Analysis of catalytic pyrolysis of municipal solid waste and paper sludge using TG-FTIR, Py-GC/MS and DAEM (distributed activation energy model), Energy, 2018, 143: pp. 517-532

[16] Liu, J.; Huang, L.; Sun, G. et al.: (Co-)combustion of additives, water hyacinth and sewage sludge: Thermogravimetric, kinetic, gas and thermodynamic modeling analyses, Waste Management, 2018, 81: pp. 211-219